Supporting Information

Ultra-high capacity and selectively immobilization of Pb through crystal growth of hydroxypyromorphite on amino-functionalized hydrochar

Yali Chen, [a] Jiejie Chen, [a] Siqin Chen,[a] Ke Tian and Hong Jiang[a*]

CAS Key Laboratory of Urban Pollutant Conversion, Department of Chemistry, University of Science and Technology of China, Hefei 230026, China

Table S1 Physical Characteristics of AFHC.

parameters	units	AFHC
BET surface area	$m^2 g^{-1}$	32.9612
total pore volume	$cm^2 g^{-1}$	0.133213
adsorption average pore width	Å	161.6603

Table S2 Elemental Composition of PHC and AFHC.

parameters	units	AFHC	PHC
C	%	33.2	66.3
H	%	3.2	5.1
O	%	20.8	26.0
N	%	10.1	3.6
P	%	13.1	ND[a]
Ca	%	7.0	ND
Mg	%	6.6	ND

ND[a]=not detected.

Table S3 Relative content of surface groups determined by N 1s, and C 1s spectra from XPS for pristine hydrochar and amino-functionalized hydrochar.

Hydrochar (atomic conc. %)	Surface concentration from N 1s peak of (at. %)			
	Pyridinic-N	Amides-N	Pyrrole-N	Pyridine-N-oxide
PHC (3.04)		0.99	1.73	0.32
AFHC (9.28)	2.82	4.02	2.44	
	Surface concentration from C 1s peak of (at. %)			
	C=C	C-C	C-OH	
PHC (78.81)		27.18	51.63	
AFHC (45.22)	12.17	17.58	15.47	

Table S4 Maximum adsorption capacity of Pb (II) ions on various adsorbents.

adsorbent	adsorption conditions	q_{max} (mg g^{-1})	reference
activated carbons	298 K, 40 min, pH=6.0	118.8	[s1]
activated carbon cloths	293 K, 12 h, pH=5.0	30.5	[s2]
carbon nanotubes	298 K, 2 h, pH=5.0	454.5	[s3]
peanut hull hydrochar	RT[a], 24 h	22.8	[s4]
attapulgite clay@carbon	RT, 40 min, pH=6.0	263.8	[s5]
pinewood hydrochar	318 K, 24 h, pH=5.0	4.25	[s6]
biochar-ealginate capsule	RT, 4 h, pH=5.0	263.1	[s7]
EDTA-graphene oxide	298 K, 24 h, pH=6.8	525.0	[s8]
few-layered graphene oxide	293 K, 24 h, pH=6.0	842.0	[s9]
fungus biomass	323 K, 210 min, pH=5.0	208.3	[s10]
CaCO3-PEI NRs	RT, 30 min, pH=4.0	240	[s11]
NV-PEI	RT, 16 min, pH=6.0	2762	[s12]
AFHC	298 K, 30 min, pH=4.0	1114.5	this work

RT[a]: room temperature.

Table S5 Removal efficiencies of AFHC for toxic metal ions of lead, zinc and cadmium in different experimental systems (Pb only, Zn only, Cd only, Pb/Zn, Pb/Cd, and Pb/Zn/Cd).

Meatal Ion	Experimental System	Initial Conc. (ppm)	Equilibrium Conc. (ppm)	% Removal
Pb	Pb/Zn	100.45	4.55	95.47
	Pb/Cd	105.53	6.61	93.74
	Pb/Zn/Cd	97.58	3.73	96.18
Zn	Zn only	32.38	26.68	17.60
	Pb/Zn	32.05	25.33	20.97
	Pb/Zn/Cd	31.85	29.63	6.97
Cd	Cd only	66.45	53.61	19.32
	Pb/Cd	65.76	51.51	21.67
	Pb/Zn/Cd	58.85	52.93	10.06

Table S6 Removal efficiencies of toxic metal ions (lead and copper) by AFHC in different experimental systems (Pb only and Pb/Cu)

Metal Ion	Experimental System	Initial Conc. (ppm)	Equilibrium Conc. (ppm)	%Removal
Pb	Pb only	105.06	7.54	92.82
	Pb/Cu	100.52	6.40	93.63
Cu	Pb/Cu	46.35	36.75	20.71

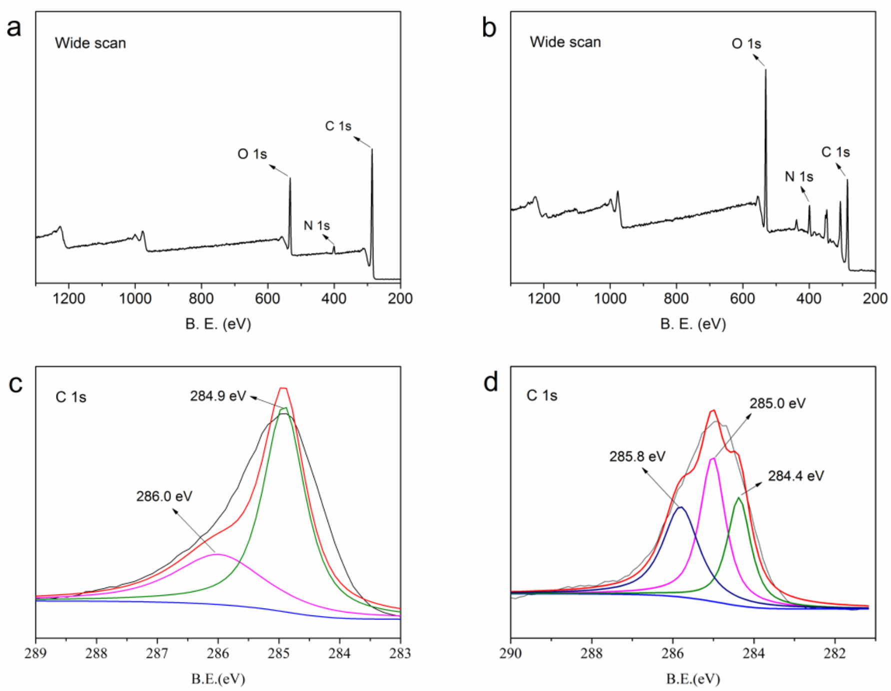

Fig. S1. XPS wide scan spectra of PHC (a) and AFHC (b). XPS spectra of C 1s for PHC (c) and AFHC (d).

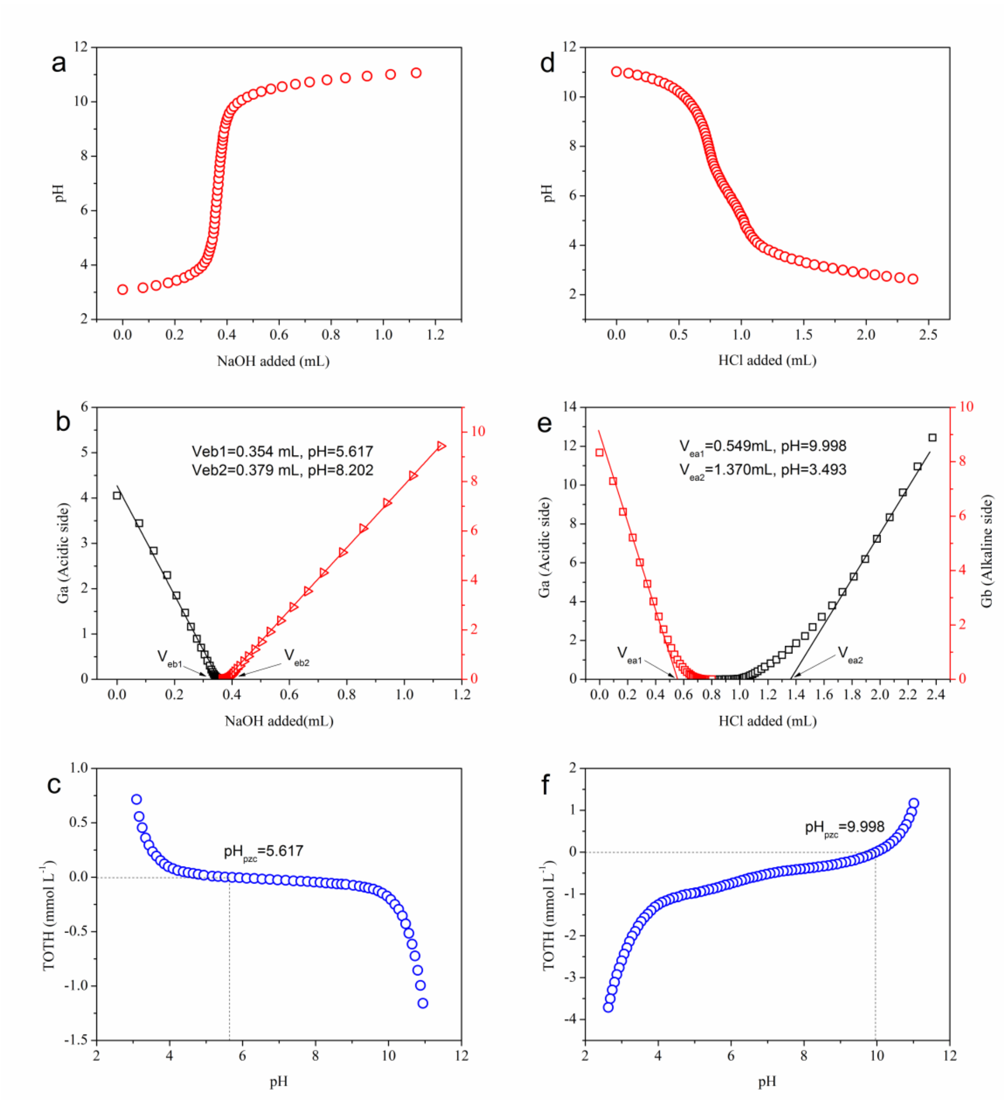

Fig. S2. Acid-base titration curve for the PHC (a) and AFHC solution (d), Gran plots for titration of PHC (b) and AFHC (e), and the point of zero charge value of PHC (c) and AFHC (f).

Figure S2b and e shows the Gran plot of the back-titration data of the hydrochars. The values of the Gran function (G) were calculated as:[S13]

On the acidic side: $G_a = (V_0 + V_{at} + V_a) \times 10^{-pH} \times 100$ (1)

On the alkaline side: $G_b = (V_0 + V_{at} + V_a) \times 10^{-(13.8-pH)} \times 100$ (2)

where V_0 represents the initial volume of the suspension. V_{at} and V_a are the total volume of base solution and of H^+ added at the different titration points, respectively. The hydrogen ions added to AFHC suspension were consumed by the following steps reflected in the Gran plots: neutralization of excess OH^- in the suspension (before V_{ea1}), reactions with the functional groups on amino-functionalized hydrochar surfaces (between V_{ea1} and V_{ea2}), and adjustment of the total system pH (after V_{ea2}). An obvious difference between V_{ea1} and V_{ea2} was found for the AFHC titration, suggesting that AFHC has a certain degree of buffering capacity in acid or base systems.[S14]

The acid–base titration data and fitting curve of PHC are shown in Fig. S2c. *TOTH* is the total concentration of consumed protons in the titration process, which is calculated from the following equation:

$$TOTH = \frac{-(V_{\mathrm{a}} - V_{ea1}) \cdot C_a}{V_0 + V_a} \qquad (3)$$

where C_a is the concentration of HCl used in the acid–base titration.

The typical acid–base titration curve of AFHC is shown in Fig. S2d. The reverse S-shaped titration curve was further transferred into two straight lines, which were disconnected at the end points (Fig. S2e) using a mathematical method proposed by Gran.[S13] The point of zero charge (pH_{pzc}) value of AFHC was 10.0 which obtained when the *TOTH* equal to zero (point of zero charge of PHC was 5.6). The surface chemical property of AFHC was alkaline, whereas the PHC was acidic, which ascribes to the increased content of nitrogen and nitrogen functional groups and the decreased content of hydroxyl and carboxyl in the process of synthesize AFHC (according to element analysis, FTIR, XPS N 1s results).

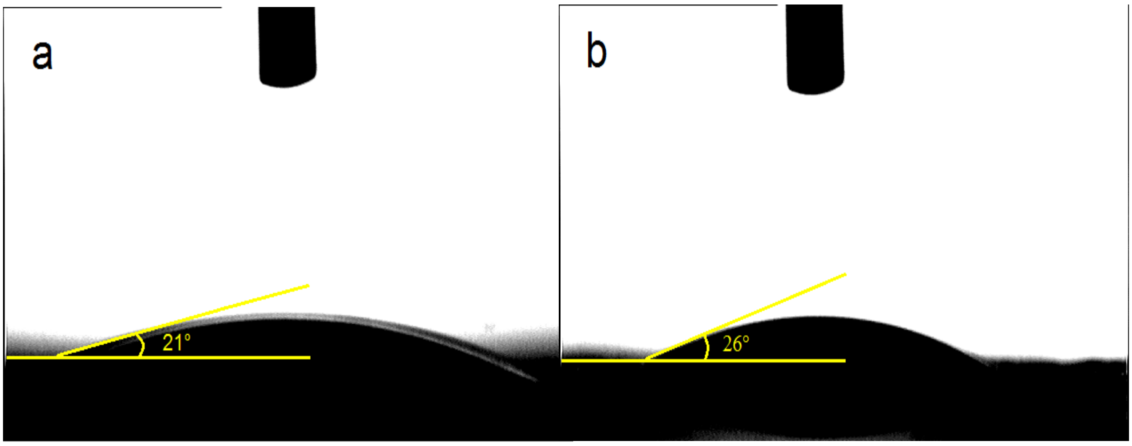

Fig. S3. Deinonized water contact angle images of PHC (a) and AFHC (b).

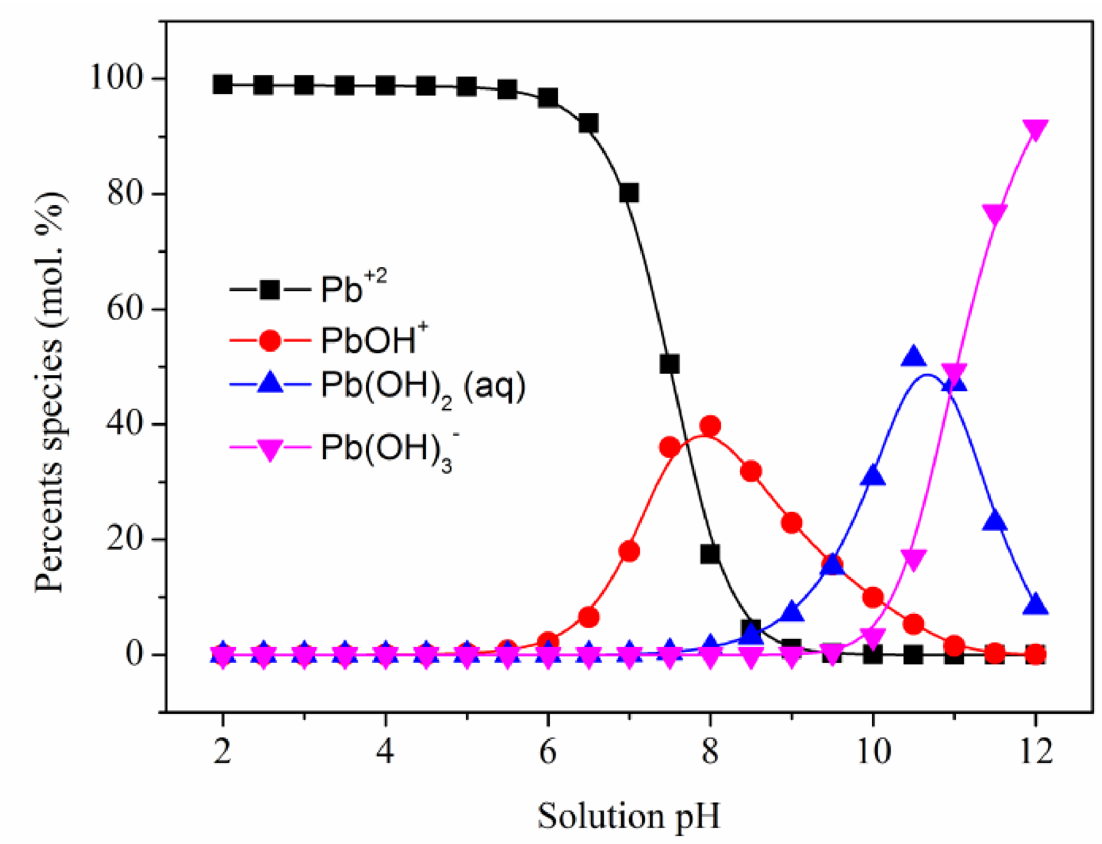

Fig. S4. Speciation distribution of Pb (II) in aqueous solution of different pHs.

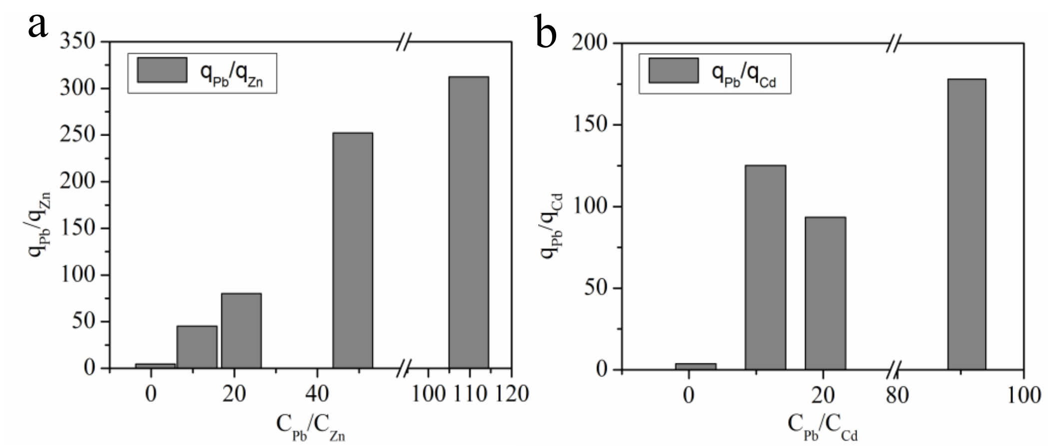

Fig. S5. The ratios of adsorption capacities of Pb and Zn (or Cd) at different concentration ratios of Pb and Zn (or Cd).

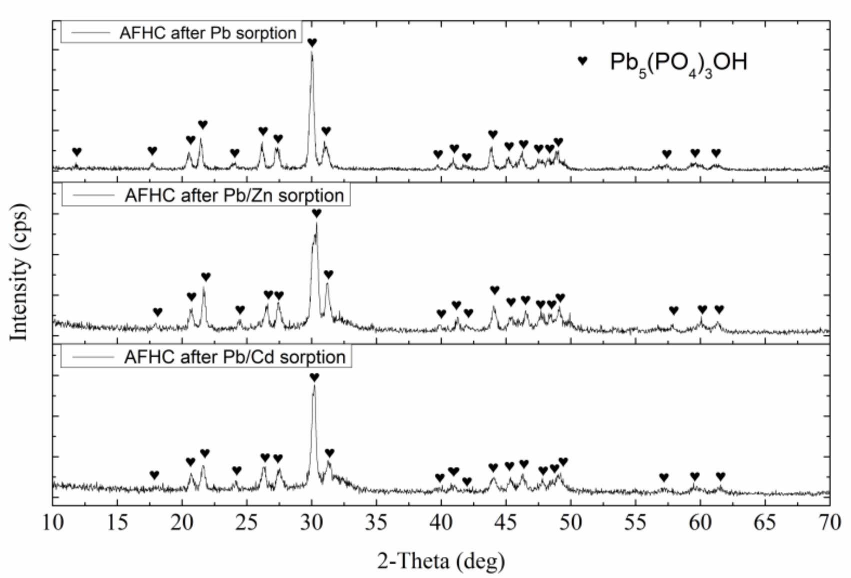

Fig. S6. XRD spectra of AFHC after Pb, Pb/Zn and Pb/Cd sorption.

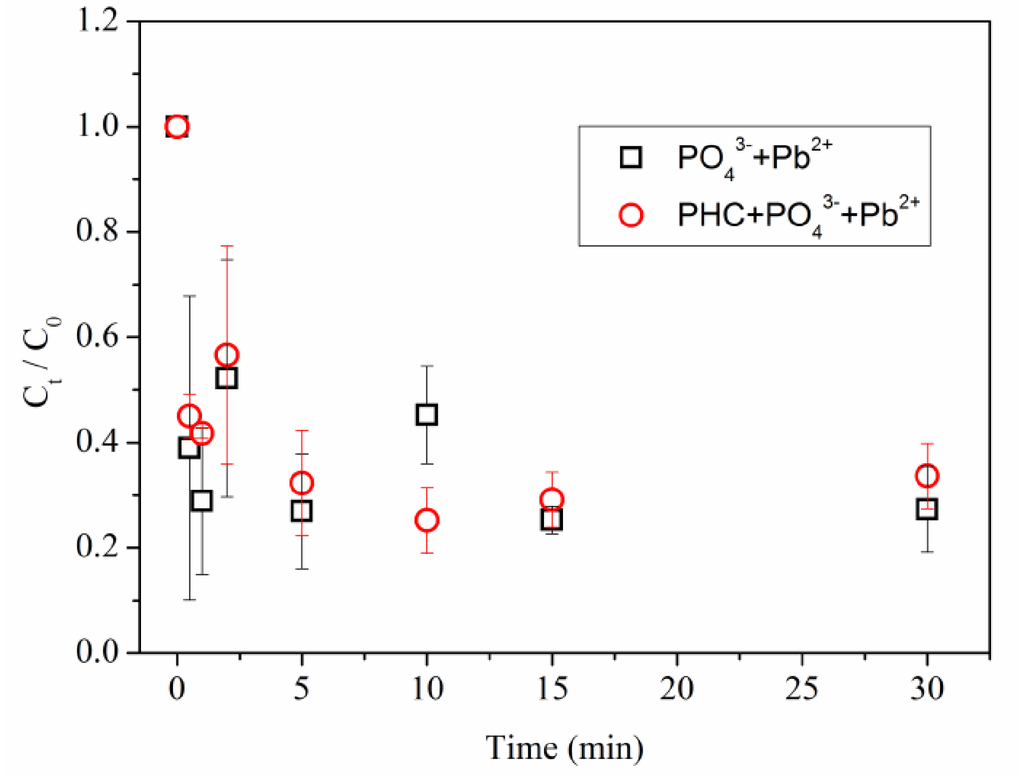

Fig. S7. Pb removal control experiments. Experiment conditions: 10 mg PHC +30 mg L^{-1} P (KH_2PO_4) + 50 mL 100 mg L^{-1} Pb^{2+}, 25℃, 180 rpm.

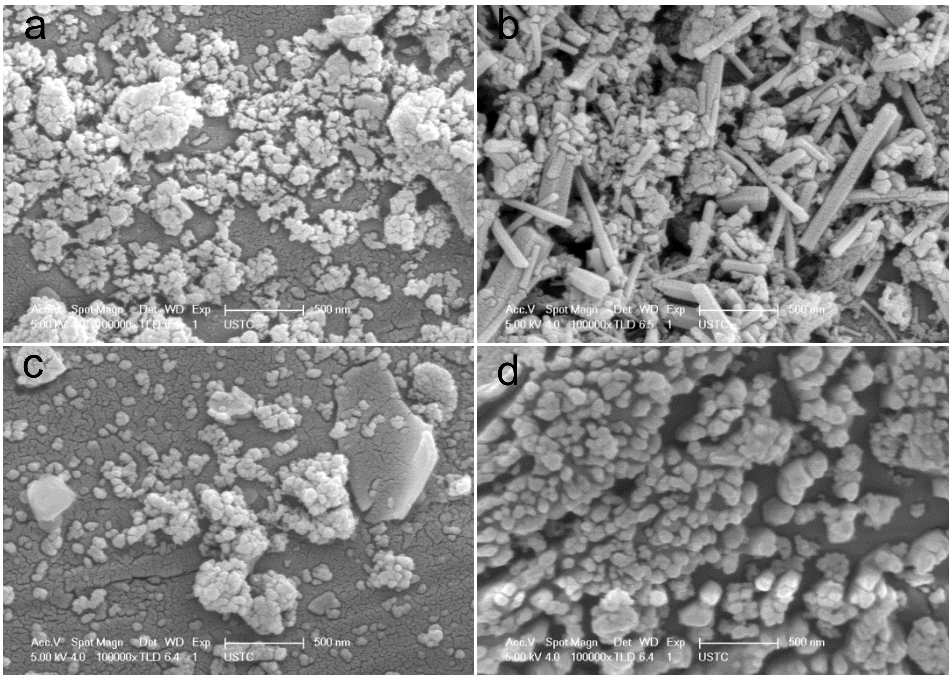

Fig. S8. SEM images of AFHC before (a) and after Pb (b), Cd (c), Zn (d) sorption.

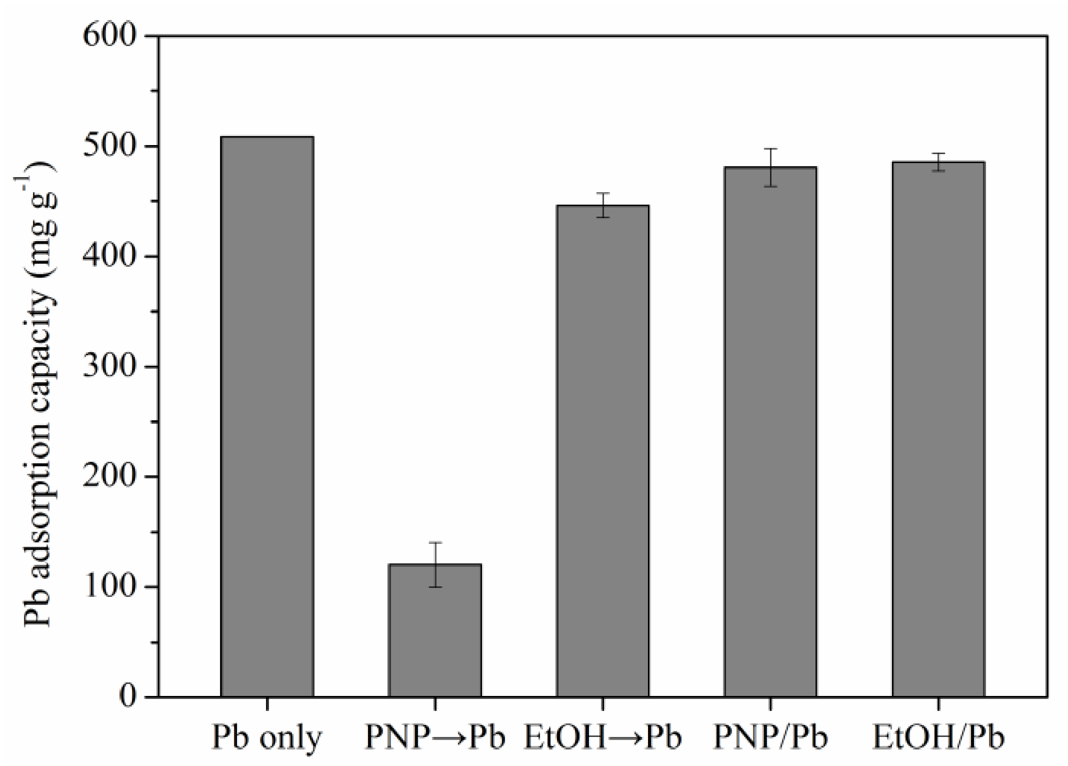

Fig. S9. The effects of organic compounds on Pb adsorption

References

[S1] Y.Huang, S.Li, J.Chen, X.Zhang, Y.Chen, *Appl. Surf. Sci.* **2014**,*293*, 160.

[S2] K.Kadirvelu, C.Faur-Brasquet, P. L.Cloirec, *Langmuir* **2000**,*16*, 8404.

[S3] Ş. S.Bayazit, İ.İnci, *J. Ind. Eng. Chem.* **2013**,*19*, 2064.

[S4] Y.Xue, B.Gao, Y.Yao, M.Inyang, M.Zhang, A. R.Zimmerman, K. S.Ro, *Chem. Eng. J.* **2012**,*200–202*, 673.

[S5] L.F.Chen, H.W.Liang, Y.Lu, C.H.Yu, S.H.Cui, *Langmuir* **2011**,*27*, 8998.

[S6] Z.Liu, F.S.Zhang, *J. Hazard. Mater.* **2009**,*167*, 933.

[S7] X.H.Do, B.K.Lee, *J. Environ. Manage.* **2013**,*131*, 375.

[S8] C. J.Madadrang, H. Y.Kim, G.Gao, N.Wang, J.Zhu, H.Feng, M.Gorring, M. L.Kasner, S.Hou, *ACS Appl. Mater. Interf.* **2012**,*4*, 1186.

[S9] G.Zhao, X.Ren, X.Gao, X.Tan, J.Li, C.Chen, Y.Huang, X.Wang, *Dalton transactions* **2011**,*40*, 10945.

[S10] M. V.Subbaiah, G.Yuvaraja, Y.Vijaya, A.Krishnaiah, *J. Taiwan Inst. Chem. Eng.* **2011**,*42*, 965.

[S11] A. M. López_Marzo, J. Pons and A. Merkoçi, J. Mater. Chem. A 2014, 2, 8766-8772.

[S12] A. M. López_Marzo, J. Pons and A. Merkoçi, J. Mater. Chem. A 2013, 1, 13532-13541.

[S13] Z.Niu, Q.Fan, W.Wang, J.Xu, L.Chen, W.Wu, Appl. Radiat. Isotopes 2009, 67, 1582.

[S14] L.L.Wang, L.F.Wang, X.M.Ren, X.D.Ye, W.W.Li, S.J.Yuan, M.Sun, G.P.Sheng, H.Q.Yu, X.K.Wang, *Environ. Sci. Technol.***2011**,*46*, 737.